Journal of Fluorescence, Vol. 4, No. 4, 1994

Surface Area per Molecule in Lipid/$C_{12}E_n$ Membranes as Seen by Fluorescence Resonance Energy Transfer

G. Lantzsch,[1] H. Binder,[1] and H. Heerklotz[1]

Received October 18, 1993

Fluorescence resonance energy transfer (FRET) from NBD-PE to rhodamine-PE has been used to measure the average area occupied by surfactant molecules in lipid bilayers. The Foerster radius has been determined from the spectral overlap of donor fluorescence and acceptor absorption (R_0 = 4.6 nm). The results of steady-state as well as of time-resolved investigations have been compared. The analysis of time-resolved fluorescence data by means of nonexponential decay functions yields an average area per lipid of 0.65 nm² in pure POPC bilayers. The area per surfactant in two-component $C_{12}E_n$/POPC-membranes (n = 2, 4, 6) has been determined and compared with the results of X-ray investigations. The surfactant head group seems to adapt a predominantly disordered confirmation within the bilayer.

KEY WORDS: Lipid membrane; $C_{12}E_n$; fluorescence resonance energy transfers; surface area.

INTRODUCTION

Lipid/detergent mixtures are of interest for technical purposes (e.g., membrane reconstitution [1,2], protein isolation [3]) as well as for fundamental membrane interaction processes. For example, to study the physical basis of hydration forces between membrane surfaces [4–7], lipid bilayers have been modified by incorporation of nonionic surfactants $C_{12}E_n$ [8]. The detailed interpretation of experimentally found hydration forces requires the knowledge of the detergent-induced structural and dynamic changes of the membrane. These changes depend on the conformation of the eto "headgroups" in the mixed membrane. The investigation of the average area occupied by one surfactant molecule in the lateral plane of the membrane allows us to distinguish between the possible conformations of the eto chain reported in the literature [9–11].

Fluorescence resonance energy transfer (FRET) normally takes place over distances up to several nanometers. Therefore it represents an ideal choice to investigate geometrical relations in molecular aggregates such as lipid membranes. We have used two fluorescent labeled lipids as energy donor (NBD-PE) and acceptor (rhodamine-PE) to determine the surface area per surfactant molecule in two-component $C_{12}E_n$/POPC membranes (n = 2, 4, 6) at different compositions.

MATERIALS AND METHODS

The lipid 1-palmitoyl-2-oleoyl-*sn*-glycero-3-phosphatidyl-choline (POPC) and the fluorescent egg phosphatidylethanolamine derivates NBD-PE and rhodamine-PE were purchased from Avanti Polar Lipids, the oligoethylenglycol-dodecyl ether ($C_{12}E_n$; n = 2, 4, 6) was from Nikko Chemicals Co. (Japan) and the 1,6-diphenyl-1,3-hexatriene (DPH) was from Serva (Germany). The substances are of a purity >99% and were used without further purification.

Lipid vesicles were prepared as follows: Stock solutions of all substances in methanol (spectroscopic

[1] Universität Leipzig, FB Physik, Linnéstrasse 5, 04103 Leipzig, Germany.

1053-0509/94/1200-0339$07.00/0

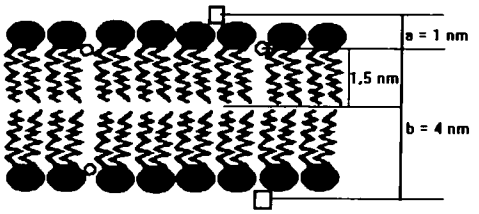

Fig. 1. Localization of the fluorescent probes NBD-PE- (○) and rhodamine-PE (□) in the POPC membrane (schematically).

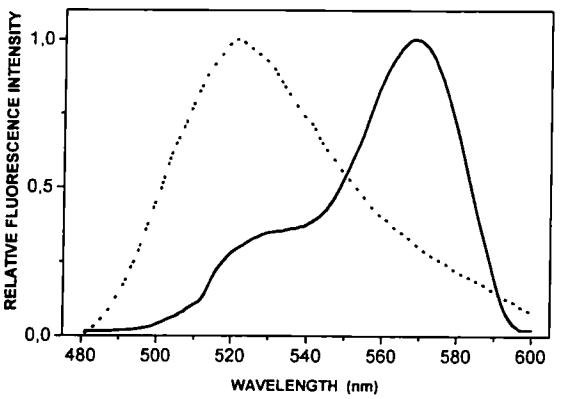

Fig. 2. Emission spectrum of the donor, NBD-PE (---), and absorption spectrum of the acceptor, Rh-PE (——), in POPC vesicles (at a molar ratio of 1:200, probe to lipid) at 25°C.

grade) were mixed in definite relations and dried under vacuum at room temperature. After the addition of triple-distilled water the samples were rapidly vortexed two times for 1 min each and stored overnight under nitrogen at 4°C. To control the amount of unilamellar vesicles, in some cases samples were prepared additionally by the extrusion technique [12] to produce unilamellar vesicles with a very narrow size distribution about the diameter of the filter pores (100 nm) as controlled by quasielastic light scattering measurements. No significant differences in fluorescence data obtained from both preparations were detected. We concluded the simpler first procedure to be sufficient for preparation of lipid dispersions of unilamellar vesicles and used it as the standard technique.

The concentrations of POPC and NBD-PE within the samples were adjusted to 500 and 2.5 μM, respectively. The molar ratio Rh-PE:POPC, x_A, was varied between 0.001 and 0.02 to give a remarkable effect of FRET. The acceptor concentration within the sample was controlled by absorption spectroscopy.

The steady-state emission spectra were recorded on a Perkin–Elmer LS50 spectrometer and the fluorescence decays on a N_2-laser impulse spectrometer LIF 200 (ZWG Berlin). Decay curves were analyzed by means of a nonlinear iterative fitting algorithm including deconvolution of the measured excitation pulse with the respective model function. Usual test criteria were applied to check the quality of the fits. For time-resolved fluorescence anisotropy measurements, DPH was used at a molar ratio DPH:POPC of 0.002. Parallel and perpendicular polarized fluorescence intensity decays of DPH were measured. The anisotropy decays were analyzed by means of the model developed by Kinosita *et al.* [13] to obtain the limiting values of the anisotropy at $t = 0$, t_0 and $t >> \tau_0$, r_∞ as described in Ref. 14. The orientational order parameter of the fluorophore has been calculated by means of Eq. (1) [15]:

$$S = \sqrt{\frac{r_\infty}{r_0}} \tag{1}$$

FRET IN LIPID MEMBRANES

We assume the energy donors and acceptors to be located at definite depths within the membrane and to be distributed randomly over the layer. Thus, donors transfer excitation energy to acceptors within the same monolayer as well as to those within the opposite one. The rate of FRET depends on the separations between the donor and the acceptor layers, a and b (see Fig. 1), the two-dimensional acceptor concentration C_A (acceptors per nm^2), and the Foerster radius,

$$R_0 = 9.768 \cdot 10^3 \cdot (K^2\, Q_n\, n^{-4}\, J_{DA})$$

with $n = 1.4$, the refractive index of the medium, and $K^2 = 2/3$, the dipole–dipole orientation factor for randomly oriented fluorophores. The quantum yield of the donor in the samples without acceptor, $Q_D = 0.27 \pm 0.3$, was determined using quinine sulfate as standard ($Q = 0.55$). The overlap integral, J_{DA}, was calculated from the fluorescence and absorption spectra of NBD-PE and rhodamine-PE, respectively (Fig. 2) to give the critical radius $R_0 = (4.6 \pm 0.1)$ nm.

After delta pulse excitation the donor fluorescence decays nonexponentially according to the model function

$$i(t) = i_0(t) \cdot N_D(t,a) \cdot N_D(t,b) \tag{2}$$

$i_0(t)$ denotes the fluorescence decay of the donor in the absence of FRET (with the lifetime: τ_0). $N(t,a)$ and $N(t,b)$ are functions of the form [16]

$$N_D(t,y) = \exp\{2\pi y^2 C_A \cdot$$

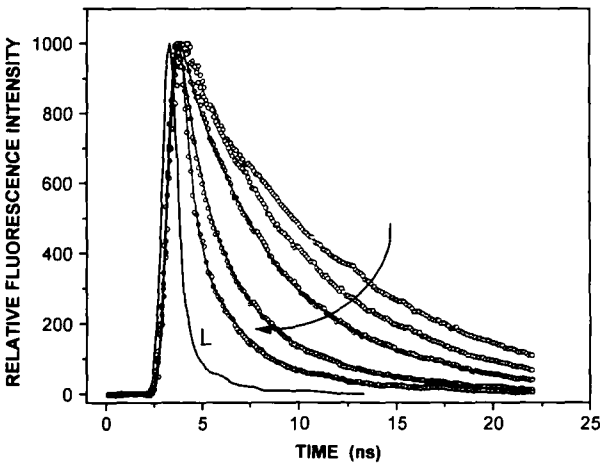

Fig. 3. Emission spectra of donor and acceptor labeled POPC vesicles at molar ratios of acceptor:lipid, $X_A * 10^2$, of 0, 0.14, 0.24, 0.56, 1.12, and 1.68, in order of decreasing signal in the donor emission region (arrow) at 25°C.

$$\int_0 (1 - \exp(-\frac{t}{\tau_0})(\frac{R_0}{y})^6\beta^6)\ \beta^{-3}d\beta\} \qquad (3)$$

describing the deactivation of the donor due to FRET to both sides of the membrane. R denotes the distance between one chosen donor molecule and an acceptor molecule. The FRET efficiency, E, is given by the equation

$$E = 1 - \frac{I}{I_0} \qquad (4)$$

with I and I_0 the fluorescence intensities of the donor in the presence and absence of the acceptor.

RESULTS AND DISCUSSION

The localization of the fluorophores in the lipid bilayer was evaluated, comparing its fluorescence spectra in lipid vesicles with those in solvents of different polarities according to Waggoner and Stryer [17]. The wavelengths of maximal fluorescence intensity in the lipid system correspond to the emission maximum in methanol (NBD-PE) and water (rhodamine-PE). Thus the fluorophore rhodamine is assumed to be located on the lipid–water interface of the membrane and, in agreement with Ref. 18, NBD within the glycerol region as shown schematically in Fig. 1.

The nonexponential decay function (2), which considers the dynamic quenching of donor fluorescence by the FRET mechanism in a bilayer, as well as a sum of three exponentials is well fitted to the time-resolved fluorescence intensities of NBD-PE (Fig. 3).

To evaluate the capabilities of steady-state and time-resolved fluorescence measurements to investigate membrane geometry, we compared FRET efficiencies [Eq. (4)] determined alternatively by means of

(i) the average intensity-weighted lifetime of standard three-exponential decay functions, i.e.,

$$I \propto \langle\tau\rangle \quad \text{with} \quad \langle\tau\rangle = \frac{\sum_{i=1}^{3} a_i \tau_i^2}{\sum_{i=1}^{3} a_i \tau_i} \qquad (5)$$

(ii) the stationary fluorescence intensity of the donor fluorescence at 520 nm, and

(iii) numerical integration of the respective nonexponential decay function (2), i.e.,

$$I \propto \int_0^\infty i(t)\ dt \qquad (6)$$

Significant deviations between the exact solution (iii) and the alternative determinations (ii) and (i) (see Fig. 5) are due to

- an inadequate description of the intensity decay outside the time window of the measurement and
- reabsorption of the donor emission by the acceptor molecules expressed in the apparent shift of the spectra to shorter wavelengths (Fig. 4). Strong dilution of the samples may prevent this inner filter effect. But decreasing the sample concentration below 500 μM leads to a significant loss of the amount of surfactant in the membrane because of its partition between water and membrane phases [19].

Thus methods (i) and (ii) are shown to be unacceptable because of systematic errors. We therefore prefer the direct analysis of the experimental fluorescence decay in terms of the nonexponential model function (2) as the best choice to investigate the geometry of the lipid bilayer. Our curve analysis seeks for a suitable acceptor concentration C_A to fit the experimental decay data. The distances between donor and acceptor layers are fixed to $a = 1$ nm and $b = 4$ nm assuming a thickness of the hydrophobic core of about 3 nm $\approx b - a$ (see Fig. 1).

In pure POPC membranes C_A is given by $C_A = x_A/A_L$, with A_L the average area occupied by one POPC molecule. Thus linear regression of the obtained C_A's versus x_A, the molar ratios of acceptor to lipid within the sample, yields $A_L \approx 0.65 \pm 0.03$ nm (Fig. 6).

In two-component lipid–surfactant bilayers the acceptor concentration is $C_A = x_A/A$. The respective area A corresponds to one lipid and $R_{S/L}$ surfactant molecules.

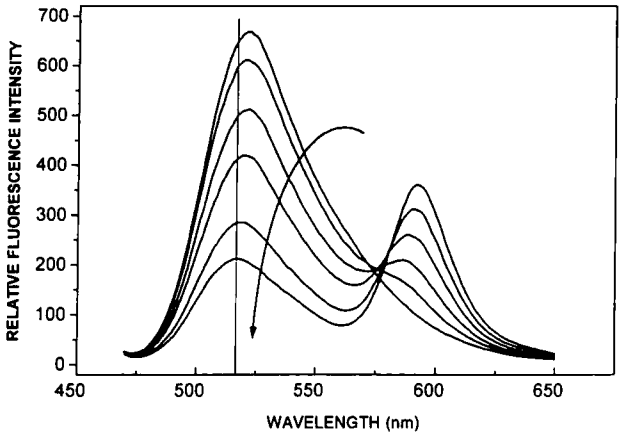

Fig. 4. Experimental donor fluorescence decays (○) in the presence of acceptor at molar ratios of acceptor:POPC, X_A * 10^2, of 0, 0.24, 0.56, 1.12, and 1.68, at 25°C; light pulse (L) and model curves calculated according to Eq. (1) (——).

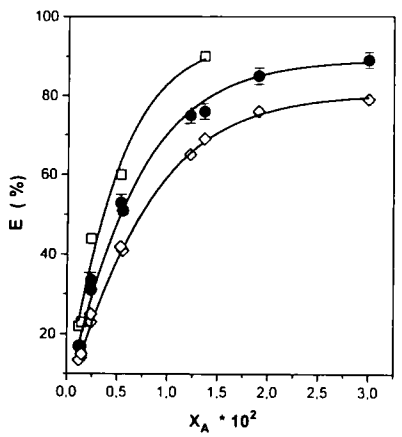

Fig. 5. FRET efficiencies, E, determined experimentally by means of steady-state intensity at 520 nm (□); three-exponential (◇) and non-exponential (●) decay analysis of the donor fluorescence at 25°C. Lines are calculated by means of Eq. (1) in POPC vesicles with a = 1 nm, b = 4 nm, and A_L = 0.45 nm², 0.65 nm², and 0.95 nm² to fit (□), (●), and (◇), respectively.

$R_{S/L}$ denotes the molar ratio of surfactant:lipid. Assuming additivity of the areas of lipids and surfactants, the net area per surfactant molecule, A_S, was calculated using the equation

$$A_S = \frac{(A - A_L)}{R_{S/L}} \qquad (7)$$

(see Table I).

At increasing concentrations of $C_{12}E_n$ this assumption seems to be critical because of a continuous fluidization of the membrane. Fluidization should result in an increasing area per lipid, accompanied by a decreasing membrane thickness [5].

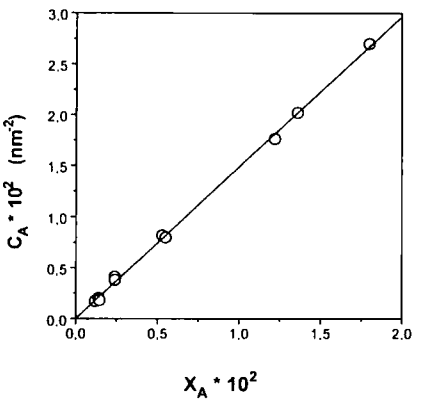

Fig. 6. Acceptor concentration C_A versus molar ratio of acceptor:lipid, X_A (* 10^2). C_A was obtained from the decay analysis by means of Eq. (1) of donor fluorescence in POPC vesicles at 25°C. Linear regression yields A_L = 0.65 nm².

Table I. The Net Area per Surfactant Molecules (nm²) in POPC and POPC/Surfactant Membranes Determined by FRET and X-Ray Diffraction [20]

	Fluorescence			X-Ray
			0.65 ± 0.03	0.065 ± 0.02
	A_T at a molar ratio $R_{S/L}$ in the mixed membrane of			
POPC	0.33	0.67	1	0.5
$C_{12}E_2$	0.28 ± 0.1	—	0.26 ± 0.03	0.26 ± 0.02
$C_{12}E_4$	0.66 ± 0.1	0.60 ± 0.07	0.45 ± 0.03	0.40 ± 0.02
$C_{12}E_6$	—	0.63 ± 0.07	0.63 ± 0.04	
$C_{12}E_8$				0.60 ± 0.02

To study the effect of membrane fluidity on the apparent area per lipid, we measured the temperature dependence of donor fluorescence decay as well as of the DPH order parameter in pure POPC dispersions. The donor fluorescence was analyzed by means of Eq. (2) using fixed donor–acceptor plane separation distances, a and b (Fig. 1), yielding the apparent molecular area. Upon raising temperature the fluidity of the hydrocarbon chains of the lipids increases continuously, which is indicated by decreasing DPH order parameter. However, the apparent molecular area remains constant within the range of experimental errors (Fig. 7).

We emphasize that the constant parameters a and b used in the numerical fit procedure would correspond to constant thickness of the headgroup and hydrocarbon regions of the membrane. Especially the latter approximation is in conflict with the expectations for increasing fluidity.

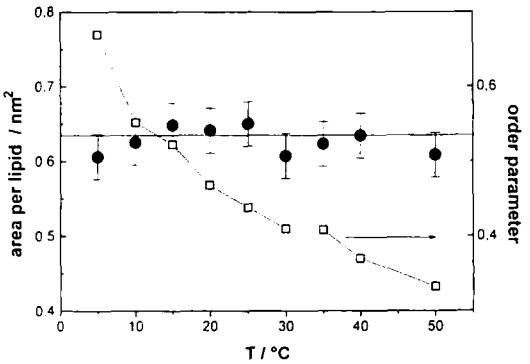

Fig. 7. Apparent area per POPC molecule (●) and DPH order parameter (□) versus temperature in pure POPC membranes. The surface area was determined assuming constant distances between donor and acceptor planes (see text).

In our case R_0 is comparable to the membrane thickness. Therefore the rate of FRET depends significantly on the average donor–acceptor distances within one monolayer as well as on those between donors and acceptors in opposite monolayers. Whereas the first will increase upon area expansion, the latter will be diminished by the accompanying reduction of hydrocarbon-region thickness. Obviously these opposed influences compensate each other to some extent, making our approach insensitive to a fluidity-driven area enhancement.

The area occupied by a $C_{12}E_2$ molecule of about 0.25 nm² agrees approximately with the cross section of a hydrocarbon chain in lamellar phases of about 0.25–0.30 nm². The distinct increase in the area, up to about 0.45–0.65 nm² in the case of $C_{12}E_4$ and $C_{12}E_6$, is caused by the influence of the additional eto units. Comparing the effective cross sections of a completely disordered with that of an extended eto chain containing 4–6 units (about 0.50–0.70 nm² [9] versus 0.19 nm² [10]), a predominantly disordered conformation of the eto group of the surfactants within the lipid membranes can be concluded.

Good agreement of the molecular areas obtained from our FRET measurements and those from X-ray investigations [20,21] has been achieved in pure POPC membranes and $C_{12}E_2$-POPC mixtures. In the respective $C_{12}E_4$ and $C_{12}E_6$ systems the fluorescence method gives A_s values about 30% higher than those in the X-ray scattering experiment. Possible reasons are (i) an increased thickness of the headgroup region of the bilayer, leading to a greater average separation between the donors and the acceptors and thus to a decreased FRET efficiency, and (ii) slight differences in the membrane morphology due to the very different lipid concentration within the samples ($5 \cdot 10^{-4}$ vs 1 *M*).

CONCLUSIONS

FRET represents an alternative method to investigate the geometry of lipid membranes. To extract relevant data the measured fluorescence decays have to be analyzed directly by means of a "physical," nonexponential model function. The interpretation of the slight discrepancies between the results of X-ray and those of FRET studies as well as the behavior of other $C_{12}E_n$ derivatives will be the object of further investigations.

ACKNOWLEDGMENTS

This work was supported by the Deutsche Forschungsgemeinschaft (SFB 294).

REFERENCES

1. M. Ollivon, O. Eidelman, R. Blumenthal, and A. Walter (1988) *Biochemistry* **27**, 1695–1703.
2. J.-L. Rigaud, M.-T. Paternostre, and A. Bluzat (1988) *Biochemistry* **27**, 2677–2688.
3. D. A. Haugen and M. J. Coon (1976) *J. Biol. Chem.* **251**, 7929–7939.
4. R. P. Rand and V. A. Persegian (1989) *Biochim. Biophys. Acta* **988**, 351–376.
5. G. Cevc and D. Marsh (1987) *Phospholipid Bilayers: Physical Principles and Models*, Wiley, New York.
6. J. N. Israelachvili and H. Wennerström (1991) *J. Phys. Chem.* **96**, 520–531.
7. D. Needham, T. McIntosh, and D. Lasic (1992) *Biochim. Biophy. Acta* **1108**, 40–48.
8. F. Volke, S. Eisenblätter, J. Galle, and G. Klose (1994) *Chem. Phys. Lipids* (in press).
9. C. Tanford, Y. Nozaki, and M. F. Rohde (1977) *J. Phys. Chem.* **81**, 1555–1563.
10. M. Rösch (1972) *Tenside* **9**, 23–31.
11. M. J. Schick (1962) *J. Coll. Sci.* **17**, 801.
12. M. J. Hope, M. B. Bally, G. Webb, and P. R. Cullis (1985) *Biochim. Biophys. Acta* **812**, 55–65.
13. K. Kinosita, Jr., S. Kawato, and A. Ikegami (1977) *Biophys. J.* **20**, 289–305.
14. H. Binder, G. Lantzsch, and K. Dittes (1989) *Wiss. Z. Karl-Marx-Univ. Math.-nat. wiss. Reihe* **38**(6), 569–578.
15. F. Jähnig (1979) *Proc. Natl. Acad. Sci. USA* **76**, 6361–6365.
16. P. K. Wolber and B. S. Hudson (1979) *Biophys. J.* **28**, 197–210.
17. A. S. Waggoner and L. Stryer (1970) *Proc. Natl. Acad. Sci. USA* **67**, 579–585.
18. A. Chattopadhyay and E. London (1987) *Biochemistry* **26**, 39–44.
19. H. Heerklotz, H. Binder, and G. Lantzsch (1994). *J. of Fluorescence* **4**, 349–352.
20. B. König (1992) thesis, University of Leipzig, Leipzig.
21. G. Klose, B. König, H. W. Meyer, G. Schulze, and G. Degovics (1988) *Chem. Phys. Lipids* **47**, 225–234.